Direct observation of amophization in load rate dependent nanoindentation studies of crystalline Si

C. R. Das,[1] S. Dhara,[2,a)] Yeau-Ren Jeng,[3] Ping-Chi Tsai,[3] H. C. Hsu,[4,b)] Baldev Raj,[1,2] A. K. Bhaduri,[1] S. K. Albert,[1] A. K. Tyagi,[2] L. C. Chen,[5] and K. H. Chen[5,6]
[1]*Materials Technology Division, Indira Gandhi Centre for Atomic Research, Kalpakkam 603102, India*
[2]*Surface and Nanoscience Division, Indira Gandhi Centre for Atomic Research, Kalpakkam 603102, India*
[3]*Department of Mechanical Engineering, National Chung Cheng University, Chia-Yi 62102, Taiwan*
[4]*Institute of Electro-Optical Science and Engineering, National Cheng Kung University, Tainan 70101, Taiwan*
[5]*Center for Condensed Matter Sciences, National Taiwan University, Taipei 106, Taiwan*
[6]*Institute of Atomic and Molecular Sciences, Academia Sinica, Taipei 106, Taiwan*

(Received 30 March 2010; accepted 28 May 2010; published online 24 June 2010)

Indentation at very low load rate showed region of constant volume with releasing load in crystalline (*c*-)Si, indicating a direct observation of liquidlike amorphous phase which is incompressible under pressure. Signature of amorphization is also confirmed from load dependent indentation study where increased amount of amorphized phase is made responsible for the increasing elastic recovery of the sample with increasing load. *Ex situ* Raman study confirmed the presence of amorphous phase at the center of indentation. The molecular dynamic simulation has been employed to demonstrate that the effect of indentation velocities has a direct influence on *c*-Si during nanoindentation processes. © *2010 American Institute of Physics*. [doi:10.1063/1.3456380]

Study of materials under pressure is always of immense interest both for electronic and mechanical properties. Material experience intense localized stresses under a rigid diamond indenter. Indentation with various indentator configurations is the most effective way for performing controlled experiments in studying pressure-induced phase transformation. These high stresses are reported for pressure-induced phase transformations to denser crystalline (*c*-) and amorphous forms in monovalently[1] and covalently bonded compound[2] semiconductors along with plastic deformation, leading to recrystallization by annihilation of dislocation in ionic bonded compound semiconductors.[3,4] Phase transformation of Si under controlled pressure is of renewed interest in the age of ion cutting and ion doping to suit microelectromechanical and nanoelectromechanical systems (MEMS and NEMS) systems.[5] The study of transformation to the high pressure phase has technological importance for having control in the precision micromachining process steps using enhancement of ductility in these systems.[6]

Along with transformation into various crystalline phases, amorphization of *c*-Si is also reported at the center of various indentors.[1,7] The observation of these phase transformations, in particular amorphization are recorded by the *ex situ* techniques like transmission electron microscopy and Raman spectroscopic studies. Changes recorded in the *in situ* resistivity measurements during indentation in *c*-Si did not reflect any serious attempt for identifying phase transition.[7] In the cutting edge technological application of Si in MEMS or NEMS activities, an *in situ* information of phase transformations will be extremely useful in case of indentation studies where controlled pressure dependent studies can be performed.

We report here a direct observation of amorphization in *c*-Si during the indentation process at a slow loading-unloading rate. *Ex situ* Raman spectroscopic measurements are carried out to substantiate our claim. Direct observation of possible phase transition in the realm of other crystalline phases of Si is also explored at higher loading-unloading rates.

Intrinsic *p*-type *c*-Si(100) substrates of 300 μm thickness are used in the present study. The samples are indented using the microindenter with a Berkovich diamond indenter (three-sided pyramid with a nominal tip radius of 50 nm and having centerline-to-face angle, $\Psi = 65.3°$). The indentation conditions are as follows: load 350–700 mN; loading-unloading rate 0.1–100 mN s^{-1}, and holding time 5 s. A LabRam HR800 (Jobin-Yvon, France) spectrometer with an automatized XY-table of acquisition is used to record the micro-Raman spectra (spatial resolution of 1 μm, limited by spot size of laser) with excitation wavelength of 632.8 nm of He–Ne laser.

Typical loading-unloading curves are shown for extremely low loading-unloading rate of 0.1 mN s^{-1} (Fig. 1) for various loads in *c*-Si substrates. In all the cases, regions of constant depth are recorded (continuous-line-encircled) in the unloading line. In a crystalline material release in load (unloading) is bound to reflect in the change in the compressed volume due to relaxation. The unloading curve behaves differently, based on mechanical response of the indented and surrounded material. The observation of constant depth while releasing of load, thus indicates a possible presence of liquidlike state for which a change in volume is not appreciated. The observation of multiple such occurrences (Fig. 1) in the unloading line with increasing load may be due to the fact that amorphization may occur randomly at the freshly created surfaces of the larger deformed volume. It can also be mentioned that number of "pop-in" dotted-line-encircled (Fig. 1) in the loading line increases with increase in the load, indicating generation of progressively increasing

a)Author to whom correspondence should be addressed. Electronic mail: dhara@igcar.gov.in.
b)While performing the Raman studies the author was postdoctoral fellow at CCMS, NTU, Taipei-106, Taiwan.

 © 2010 American Institute of Physics

Downloaded 28 Jul 2010 to 140.123.124.197. Redistribution subject to AIP license or copyright; see http://apl.aip.org/apl/copyright.jsp

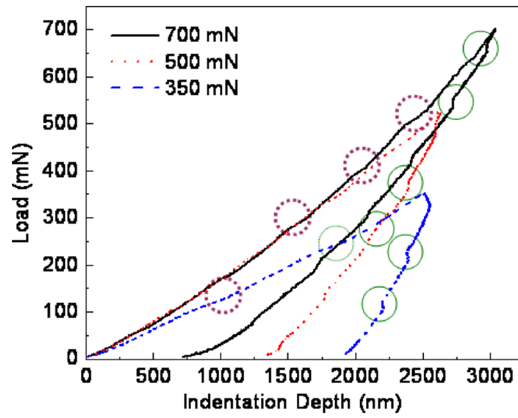

FIG. 1. (Color online) Typical loading-unloading lines at a fixed loading-unloading rate of 0.1 mN s^{-1} for various loads of 350, 500, and 700 mN. Regions of constant depth with releasing load are continuous-line-encircled in the unloading curve. Pop-in in the loading curve is also dotted-line-encircled.

number of defects in the stressed region beneath the indenter. It may be noted that no cracks were observed in the material during the tests supporting progressive increase in defects in the indented material. As a matter of fact heterogeneous nucleation of amorphization is reported in case of *c*-Si.[8] Time dependent elastic recovery in the indented sample is increases as peak load increases, as observed recoverable indentation depth increase with increasing peak load (Fig. 1). Increased amount of amorphized region with increasing load may corroborate with time depended elastic recovery of materials.[9,10]

Typical Raman line mappings for *c*-Si(100) are shown for the edge and the central regions of the indentation spot [Figs. 2(a) and 2(b)]. The indent spot (shown in the insets) is chosen for a load 700 mN and loading-unloading rate of 0.1 mN s^{-1}. The Raman mode for Si–I (0–11 GPa) phase of *c*-Si at 521 cm^{-1} along with zone boundary peak at 300 cm^{-1} are shown for the spot at a corner close to the outside region [Fig. 2(a)]. At the center of the indented spot [Fig. 2(b)], body centered cubic with eight atoms at the basis (bcc8) Si-III (10–0 GPa; 167, 382, and 437 cm^{-1}) and rhombohedral (*r*8) structure Si-XII (12–2 GPa; 183, 350, and 397) are shown [Fig. 2(b)].[11,12] At the center of the indent crystalline phase corresponding to Si-I almost disappears. A distinct broad peak around 493 cm^{-1} correspond to amorphous Si.[13,14] A less intense peak at 523 cm^{-1} is close to reported 520 cm^{-1} optical mode of bulk Si-I. Resulting stress in the central spot of indentation may cause this shift. The observation of various phases of *c*-Si under indentation in this range (5–100 mN s^{-1}) of loading-unloading rate are detailed in our earlier report using Raman line as well as area mapping studies.[13] Unlike in the present report with slow loading-unloading rate, our previous study using high loading-unloading rate showed "pop-out" [encircled in the unloading line Figs. 3(a)–3(d)] burst in the unloading line for a fixed load of 500 mN and various loading-unloading rates. These pop-outs were associated with the formation of second phase(s).[14] We must state that, irrespective of loading-unloading rate, transformation of *c*-Si into its other phases is unavoidable at the center of indentation along with the signature of amorphization.

The distribution of pressure under the indenter is given by,[15]

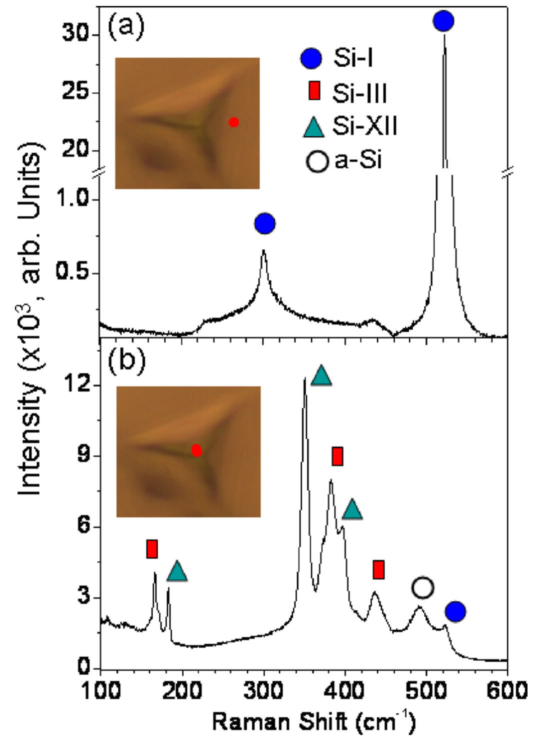

FIG. 2. (Color online) Typical Raman spectra at the (a) outside and (b) center regions, as shown in the corresponding insets of indented spot, exhibiting various phases of Si using a load of 700 mN and a loading-unloading rate of 0.1 mN s^{-1}.

$$p(r) = \frac{E}{2(1-\nu^2)} \frac{\cosh^{-1}(a/r)}{\tan \Psi}, \quad 0 \le r \le a, \qquad (1)$$

where E is Young's modulus [130 GPa for Si(100) and 185 GPa for Si(111)], ν is Poisson's ratio [0.28 for Si(100) and 0.26 for Si(111)],[16] a is the contact radius, and r is the radial coordinate in the surface. With Ψ of 65.3° in the Berkovich indenter, the pressure at the central region (for a spread of ~1 μm in the micro-Raman resolution at the center) can be calculated [Eq. (1)] as ~10 GPa (close to the boundary of ~1 μm spot at the center) to 74 GPa (close to the center). Thus Si-III and Si-XII phases are also likely to be observed

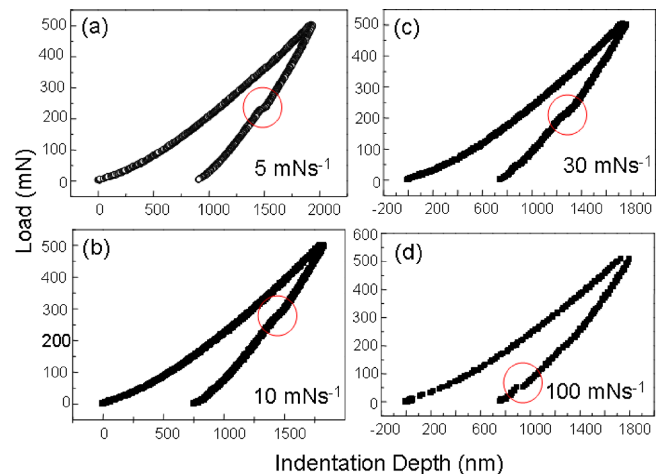

FIG. 3. (Color online) Typical loading-unloading lines at a fixed load of 500 mN and various loading-unloading rate of (a) 5 mN s^{-1}, (b) 10 mN s^{-1}, (c) 30 mN s^{-1}, and (d) 100 mN s^{-1} in *c*-Si(100) substrate. The encircled regions in the unloading curve are called as pop-out burst.

Downloaded 28 Jul 2010 to 140.123.124.197. Redistribution subject to AIP license or copyright; see http://apl.aip.org/apl/copyright.jsp

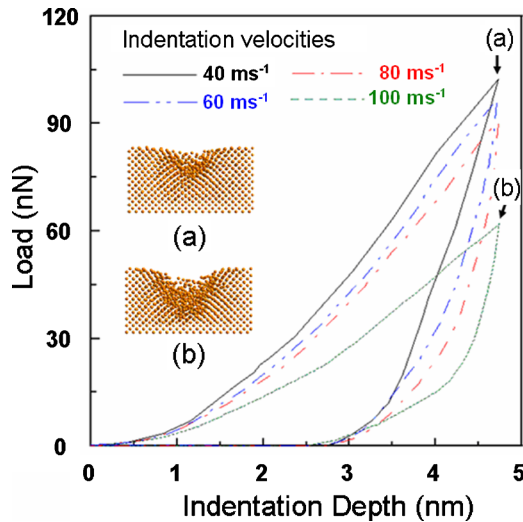

FIG. 4. (Color online) Variation in force with displacement for silicon films at various indentation velocities of $V=40$, 60, 80, and 100 ms^{-1}. Snap shots of the simulation indicating different stages of deformation (a) and (b). Corresponding load-unload curves are also indicated.

at the center of the indent spot [Fig. 2(a)].[8,11] The estimated pressure requirement, of 24 GPa for the amorphization of Si at room temperature,[7] is also provided at the center of the indent and the near-by regions [Fig. 2(b)].

In order to examine the influences of strain rates on the mechanical properties of the silicon film under nanoindentation, the simulations are performed using various indentation velocities ranging from 40 to 100 ms^{-1}. The present molecular dynamic (MD) simulations adopt the Tersoff potential[17] to study mechanical properties of silicon crystal with the (111) plane on the nanoindentation by solving the Hamilton equations of motion using Gear's fifth predictor-corrector method. Meanwhile, the *NVT* model[18] is used to control the number of atoms N, the volume V, and the temperature T. Figure 4 presents four nanoindentation load-displacement curves obtained when indenting silicon samples with the different indentation velocities of $V=40$, 60, 80, and 100 ms^{-1}. It is apparent that the effect of indentation velocities has a direct effect on the initial slope of the load-displacement curves of the various silicon samples. Specifically, for a constant indentation force, the indentation depth reduces as the indentation velocity decreases, which implies that the mechanical strength of the silicon samples increases with a reducing indentation velocity. This phenomenon arises as a result of an increase in strain energies as the indentation velocity increases, creating an increasing number of dislocations [see Figs. 4(a) and 4(b)], and thereby in turn decreases the mechanical stiffness of the silicon specimen. Remarkably, Figs. 4(a) and 4(b) also shows that the crystalline phase of silicon samples transform continuously to an amorphous phase, which implies a dramatic change in atomic short-range order by application of sufficiently large strain rates. It is necessary to note that the experimental loading-unloading rate is many orders of magnitude slower than the current simulation rate, which is comparable to that used in other MD simulations. Due to the computational intensity of the congenital problem, many of these simulations were restricted to smaller model sizes or to very high loading rates, or to both. We could not catch the signature of constant volume in the unloading curve (continuous-line-encircled regions in Fig. 1) of the experimental observation. In MD simulation, the model has orderly arrangement for atomic position to be consistent with crystalline structure. In contrast, the current results show a great number of disordered atoms, which implies liquidlike behavior. However, the present MD simulations are nevertheless adequate for generating qualitative estimates.[19] Further study employing multiscale modeling systems could overcome intrinsic bottleneck in MD simulation to obtain larger model size and slower loading rate.

In conclusion, a direct observation of liquidlike phase is reported in *c*-Si under indentation at slow loading-unloading rate. Heterogeneous model of amorphization in Si is also verified along with the increasing time dependent elastic recovery of the amorphized volume with increasing load. Raman studies confirmed the amorphization of *c*-Si. Phase transition in the other crystalline phases of Si is also reported along with the evidence of the pop-out. Finally, the MD simulation has been employed to describe, qualitatively, the effect of indentation velocities on silicon samples during nanoindentation processes leading to amorphization.

[1] J. I. Jang, M. J. Lance, S. Wen, T. Y. Tsui, and G. M. Pharr, Acta Mater. **53**, 1759 (2005); M. M. Khayyat, G. K. Banini, D. G. Hasko, and M. M. Chaudhri, J. Phys. D: Appl. Phys. **36**, 1300 (2003).
[2] Z. C. Li, L. Liu, X. Wu, L. L. He, and Y. B. Xu, Mater. Sci. Eng., A **337**, 21 (2002).
[3] C. R. Das, S. Dhara, H. C. Hsu, L. C. Chen, Y. R. Jeng, A. K. Bhaduri, B. Raj, K. H. Chen, and S. K. Albert, J. Raman Spectrosc. **40**, 1881 (2009).
[4] S. Dhara, C. R. Das, H. C. Hsu, B. Raj, A. K. Bhaduri, L. C. Chen, K. H. Chen, S. K. Albert, and A. Ray, Appl. Phys. Lett. **92**, 143114 (2008).
[5] D. W. Carr, S. Evoy, L. Sekaric, J. M. Parpia, and H. G. Craighead, Appl. Phys. Lett. **75**, 920 (1999).
[6] J. Patten, R. Fesperman, S. Kumar, S. McSpadden, J. Qu, M. Lance, R. Nemanich, and J. Huening, Appl. Phys. Lett. **83**, 4740 (2003).
[7] D. R. Clarke, M. C. Kroll, P. D. Kirchner, R. F. Cook, and B. J. Hockey, Phys. Rev. Lett. **60**, 2156 (1988).
[8] S. Takeda and J. Yamasaki, Phys. Rev. Lett. **83**, 320 (1999).
[9] H. Ikeda, Y. Qi, T. Cagin, K. Samweer, W. L. Johnson, and W. A. Goddard, Phys. Rev. Lett. **82**, 2900 (1999).
[10] H. Mizubayashi, K. Takita, and S. Okuda, Phys. Rev. B **37**, 9777 (1988).
[11] J. Z. Hu, L. D. Merkle, C. S. Menoni, and I. L. Spain, Phys. Rev. B **34**, 4679 (1986).
[12] R. O. Piltz, J. R. Maclean, S. J. Clark, G. J. Ackland, P. D. Hatton, and J. Crain, Phys. Rev. B **52**, 4072 (1995).
[13] C. R. Das, H. C. Hsu, S. Dhara, A. K. Bhaduri, B. Raj, L. C. Chen, K. H. Chen, S. K. Albert, A. Ray, and Y. Tzeng, J. Raman Spectrosc. **41**, 334 (2010).
[14] V. Domnich, and Y. Gogotsi, Rev. Adv. Mater. Sci. **3**, 1 (2002).
[15] K. L. Johnson, *Contact Mechanics* (Cambridge University Press, Cambridge, 1985), p. 107.
[16] J. J. Wortman and R. A. Evans, J. Appl. Phys. **36**, 153 (1965).
[17] J. Tersoff, Phys. Rev. Lett. **61**, 2879 (1988); Phys. Rev. B **39**, 5566 (1989).
[18] J. M. Haile, *Molecular Dynamics Simulation: Elementary Method* (Wiley, New York, 1992).
[19] Y. R. Jeng, P. C. Tsai, and T. H. Fang, J. Chem. Phys. **122**, 224713 (2005).

Downloaded 28 Jul 2010 to 140.123.124.197. Redistribution subject to AIP license or copyright; see http://apl.aip.org/apl/copyright.jsp